High Power Laser Science and Engineering, (2022), Vol. 10, e22, 6 pages.
doi:10.1017/hpl.2022.12

HIGH POWER LASER SCIENCE AND ENGINEERING

RESEARCH ARTICLE

Six kilowatt record all-fiberized and narrow-linewidth fiber amplifier with near-diffraction-limited beam quality

Guangjian Wang†, Jiaxin Song†, Yisha Chen, Shuai Ren, Pengfei Ma, Wei Liu, Tianfu Yao, and Pu Zhou

College of Advanced Interdisciplinary Studies, National University of Defense Technology, Changsha 410073, China

(Received 26 March 2022; revised 10 May 2022; accepted 8 June 2022)

Abstract

In this work, an all-fiberized and narrow-linewidth fiber amplifier with record output power and near-diffraction-limited beam quality is presented. Up to 6.12 kW fiber laser with the conversion efficiency of approximately 78.8% is achieved through the fiber amplifier based on a conventional step-index active fiber. At the maximum output power, the 3 dB spectral linewidth is approximately 0.86 nm and the beam quality factor is $M_x^2 = 1.43$, $M_y^2 = 1.36$. We have also measured and compared the output properties of the fiber amplifier employing different pumping schemes. Notably, the practical power limit of the fiber amplifier could be estimated through the maximum output powers of the fiber amplifier employing unidirectional pumping schemes. Overall, this work could provide a good reference for the optimal design and potential exploration of high-power narrow-linewidth fiber laser systems.

Keywords: fiber laser; high power; narrow linewidth

1. Introduction

High-power fiber lasers are attractive laser sources in many applications, benefitting from the essential advantages of high efficiency, excellent beam quality, compact structure and convenient thermal management[1–3]. Restricted by the pump brightness, stimulated Raman scattering (SRS) effect, transverse mode instability (TMI) effect, etc., monolithic fiber lasers with near-diffraction-limited beam quality have achieved over 10-kW level output in experiments[4,5], and there is a theoretical power limit[6–8].

The coherent beam combination and spectral beam combination provide effective approaches to breaking the limitations and further promoting the output powers of fiber lasers while maintaining excellent beam quality[9–11]. In those two beam combination systems, high-power single-mode fiber lasers with narrow-linewidth are the crucial units. Nevertheless, the power scaling of narrow-linewidth fiber lasers always lags behind that of broad-linewidth fiber lasers[12–17], because extra design is required to maintain narrow-linewidth operation. Furthermore, recent experimental results reveal that narrower signal bandwidth generally means a lower TMI threshold for the same fiber amplifier[18]. Accordingly, compared to broad-linewidth fiber amplifiers, the TMI effect is a more critical issue in designing high-power narrow-linewidth fiber amplifiers.

Extensive studies have been carried out to investigate the mechanism of the TMI effect and multiple methods are proposed to suppress the TMI effect in high-power fiber amplifiers[19–22]. The common approaches to suppressing the TMI effect in traditional step-index monolithic fiber amplifiers include shifting the pump or signal wavelength to enhance the gain saturation[23], coiling the active fiber to increase the loss of higher-order modes[24] and optimizing the pump scheme[25]. Specially designed fibers have also proved to be effective to suppress the TMI effect[26–29]. As for the optimization of the pump scheme, it involves adjusting the ratios of co-pump/counter-pump powers and measuring the corresponding TMI threshold of the fiber amplifier, which introduces extra load in the test of high-power fiber amplifiers.

In this paper, we report a 6 kW all-fiberized and narrow-linewidth fiber amplifier with near-diffraction-limited beam

Correspondence to: P. Ma and P. Zhou, College of Advanced Interdisciplinary Studies, National University of Defense Technology, Changsha 410073, China. Email: shandapengfei@126.com (P. Ma); zhoupu203@163.com (P. Zhou)

†These authors contributed equally to this paper.

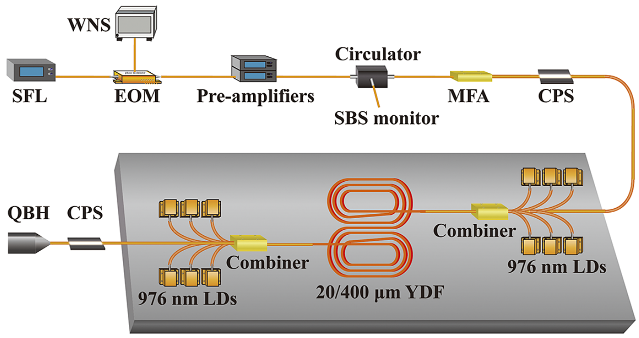

Figure 1. Experimental setup of the all-fiberized and narrow-linewidth fiber amplifier.

quality based on a conventional step-index active fiber. Up to 6.12 kW fiber laser is obtained with a conversion efficiency of approximately 78.8%. The stimulated Brillouin scattering (SBS), SRS and TMI effects are effectively suppressed at the maximum output power in the experiment. Furthermore, we have also measured and compared the output properties of the fiber amplifier employing different pumping schemes. The comparisons reveal that the output properties of the fiber amplifier employing unidirectional pumping schemes could provide practical guidance for the optimal design of high-power narrow-linewidth fiber amplifiers employing the bidirectional pumping scheme.

2. Experimental setup

The experimental setup of the high-power all-fiberized and narrow-linewidth fiber amplifier is shown in Figure 1. The fiber amplifier mainly consists of a phase-modulated single-frequency laser (SFL) serving as the seed laser and a bidirectional pumping Yb-doped fiber (YDF) amplifier. In the seed laser, an SFL at 1080 nm is first phase-modulated via an electro-optical modulator (EOM) driven by a white noise source (WNS) signal. The phase-modulated laser is then power amplified to about 50 W through the pre-amplifiers. A circulator is used after the pre-amplifiers to export the backward propagating laser from the main amplifier to protect the seed laser and monitor the SBS effect. A mode field adapter (MFA) with a 10/125 μm input fiber and 20/400 μm output fiber is used to connect the circulator and the main amplifier.

In the main amplifier, there are two sets of pump sources centering at approximately 976 nm. Each set of pump sources has six pump modules with core/cladding diameters of 220/242 μm pigtail fiber, and seven LDs with sole maximum output power of approximately 130 W and core/cladding diameters of 105/125 μm are combined by a 7×1 combiner in each module. The pump modules are injected into the conventional step-index YDF with the core/cladding diameter of 20/400 μm via two $(6+1)\times 1$ signal-pump combiners, respectively. The absorption coefficient of the YDF is approximately 1.2 dB/m at 976 nm, and the length of the YDF is approximately 14.5 m. Both ends of the YDF are coiled into a racetrack spiral shape with a minimum diameter of approximately 8.5 cm to suppress the TMI effect. Two cladding power strippers (CPSs) are used at both ends of the main amplifier to remove the residual cladding light. The main amplifier is placed on a water-cooling plate, and the final output laser is terminated through a quartz block holder (QBH).

3. Experimental results and discussion

To investigate the overall performance of the fiber amplifier, we first measure the basic output properties of the fiber amplifiers employing the forward pumping scheme and backward pumping scheme, respectively. Then, the detailed output properties of the fiber amplifier employing bidirectional pumping scheme are presented.

3.1. Output properties of the fiber amplifier employing the forward pumping scheme

Figures 2(a) and 2(b) illustrate the output power and spectral properties of the fiber amplifier employing the forward pumping scheme. As shown in Figure 2(a), the output power of the signal laser increases almost linearly with the pump power. The maximum output power is approximately 2.82 kW at the pump power of 3.69 kW, with the corresponding conversion efficiency being approximately 76.4%. In addition, there is no sign of nonlinear increase for the backward power. Thus, the SBS effect is effectively suppressed in the fiber amplifier. As shown in Figure 2(b), compared with the seed laser, the central spectrum of the signal laser at the maximum output power is nearly maintained, while the sideband of the spectrum broadens slightly. Specifically, the 3 dB spectral linewidth decreases from approximately 0.61 nm to approximately 0.33 nm, while the 20 dB spectral linewidth increases from approximately 1.58 nm to approximately 2.07 nm. In addition, the signal-to-noise ratio (SNR) exceeds 50 dB compared to the spectral component over 1100 nm, which confirms that the SRS effect is effectively suppressed in the fiber amplifier employing the forward pumping scheme. Figure 2(c) illustrates the Fourier spectrum of the signal power at the maximum output power. As shown in Figure 2(c), there is an obvious noise-like frequency distribution below 2 kHz, which indicates the occurrence of the TMI effect. Thus, further power scaling of the fiber amplifier employing the forward pumping scheme is restricted by the TMI effect.

3.2. Output properties of the fiber amplifier employing the backward pumping scheme

Figures 3(a) and 3(b) illustrate the output power and spectral properties of the fiber amplifier employing the backward

https://doi.org/10.1017/hpl.2022.12 Published online by Cambridge University Press

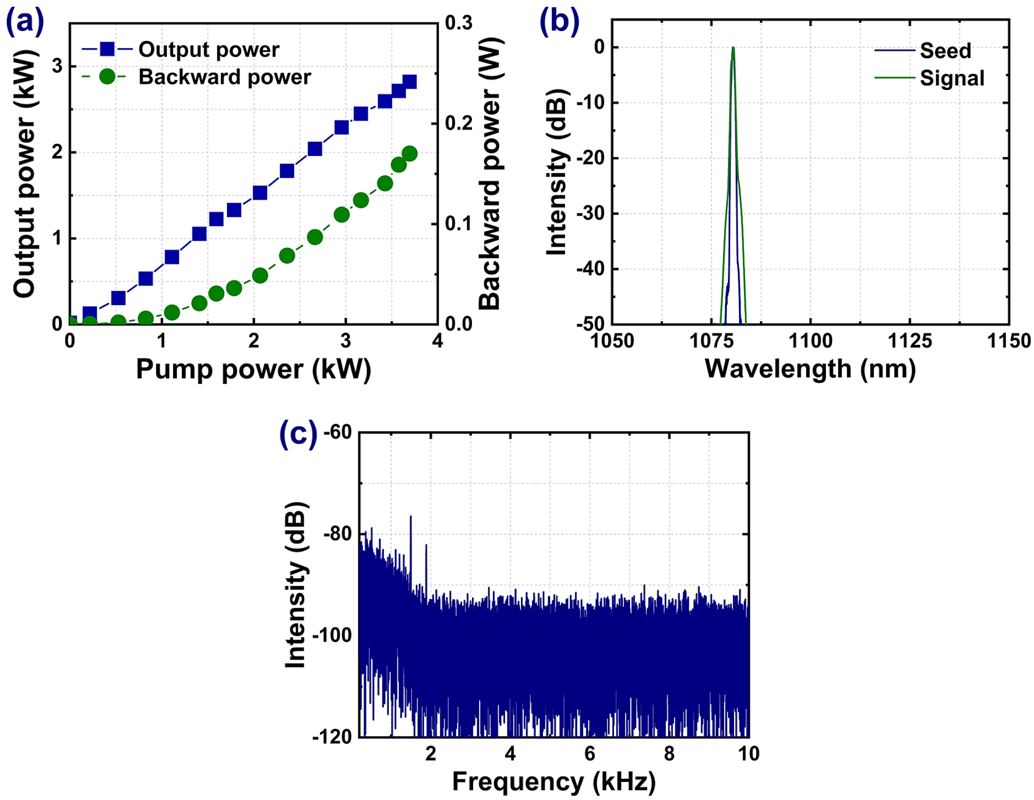

Figure 2. Basic output properties of the fiber amplifier employing the forward pumping scheme: (a) power curve; (b) output spectrum at the maximum output power; (c) Fourier spectrum of the signal laser at the maximum output power.

pumping scheme. As shown in Figure 3(a), the output power of the signal laser also increases almost linearly with the pump power. The maximum output power is approximately 3.62 kW at the pump power of 4.50 kW with the corresponding conversion efficiency being approximately 80.4%, and the SBS effect is also effectively suppressed in the fiber amplifier. As shown in Figure 3(b), the overall change of the signal laser at the maximum output power is similar to that shown in Figure 2(b). Specifically, the 3 and 20 dB spectral linewidths of the signal laser at the maximum output power are about 0.55 and 1.62 nm, respectively. In addition, the SNR also exceeds 50 dB compared to the spectral component over 1100 nm, which confirms that the SRS effect is also effectively suppressed in the fiber amplifier employing the backward pumping scheme. Figure 3(c) illustrates the Fourier spectrum of the signal laser at the maximum output power. As shown in Figure 3(c), there is obvious noise-like frequency distribution or peaks between 2 and 6 kHz, which indicates the occurrence of the TMI effect. Thus, further power scaling of the fiber amplifier employing the backward pumping scheme is also restricted by the TMI effect.

3.3. Output properties of the fiber amplifier employing the bidirectional pumping scheme

Figures 4(a) and 4(b) illustrate the output power and spectral properties of the fiber amplifier employing the bidirectional pumping scheme. As shown in Figure 4(a), the maximum output power of the signal laser could reach approximately 6.12 kW at the pump power of 7.77 kW (3.17 kW forward pump and 4.60 kW backward pump) with the corresponding conversion efficiency of approximately 78.8%, and the SBS effect is also effectively suppressed in the fiber amplifier employing the bidirectional pumping scheme. As shown in Figure 4(b), the overall changes of the output spectra near 1080 nm are similar to the results shown in Figures 2(b) and 3(b). Specifically, the 3 and 20 dB spectral linewidths of the signal laser at the maximum output power are about 0.86 and 3.98 nm, respectively. In addition, the emergence of the Raman Stokes light around 1136 nm is observed at the output power of 3.59 kW, and the intensity of the Raman Stokes light grows gradually with the increasing output power. The minimum SNR compared to the spectral component of the Raman Stokes light decreases to approximately 35.7 dB at the output power of 6.12 kW, which indicates that further power scaling of the fiber amplifier employing the bidirectional pumping scheme could be restricted by the SRS effect.

We have also measured the Fourier spectrum and the beam quality of the signal laser at the maximum output power in the fiber amplifier employing the bidirectional pumping scheme. As shown in Figure 5(a), there is no obvious noise-like frequency distribution or peaks in the Fourier spectrum,

https://doi.org/10.1017/hpl.2022.12 Published online by Cambridge University Press

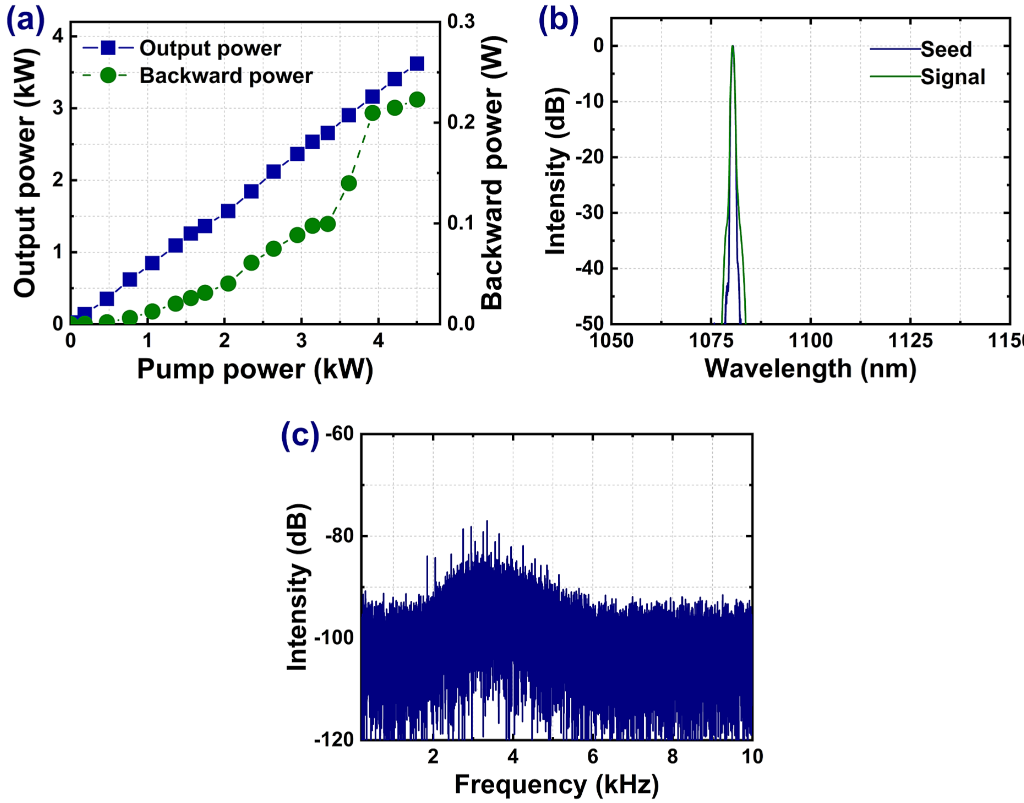

Figure 3. Basic output properties of the fiber amplifier employing the backward pumping scheme: (a) power curve; (b) output spectrum at the maximum output power; (c) Fourier spectrum of the signal laser at the maximum output power.

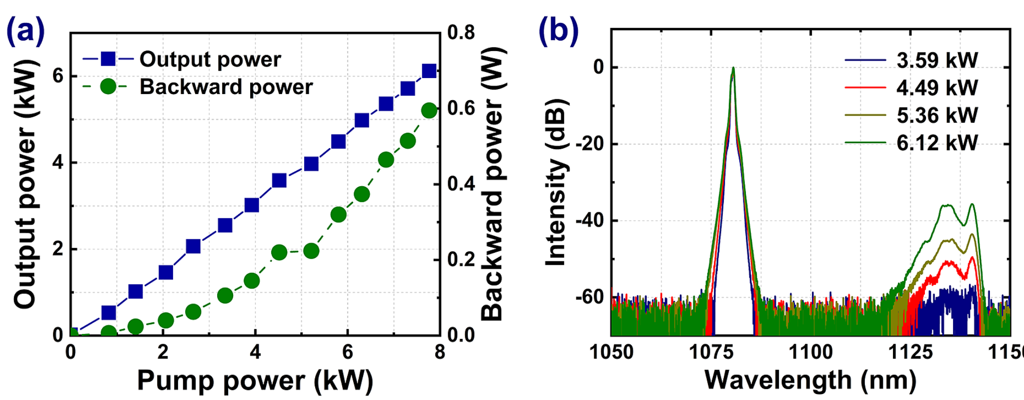

Figure 4. Basic output properties of the fiber amplifier employing the bidirectional pumping scheme: (a) power curve; (b) output spectra.

which indicates that this fiber amplifier still operates below the TMI effect at the maximum output power. The beam quality of the output laser is measured by a beam quality analyzer. As shown in Figure 5(b), the beam quality factor is measured to be $M_x^2 = 1.43$, $M_y^2 = 1.36$ at the output power of 6.12 kW, which shows that near-diffraction-limited beam quality has been achieved, and the TMI effect has been suppressed effectively. Compared with the beam quality ($M_x^2 = 1.38$, $M_y^2 = 1.28$) of the injected laser passing through the main amplifier, the beam quality is degraded a little in the power scaling process, which may be attributed to the mode distortion caused by the increased temperature of the backward pump and signal combiner in the experiment.

3.4. *Comparisons among the fiber amplifier employing different pumping schemes*

Comparing the maximum output powers of the same fiber amplifier employing different pumping schemes, we find a simple relationship among the three output powers. Specifically, the maximum output power (~6.12 kW) of the fiber amplifier employing the bidirectional pumping scheme is close (~95%) to the sum of the maximum output powers

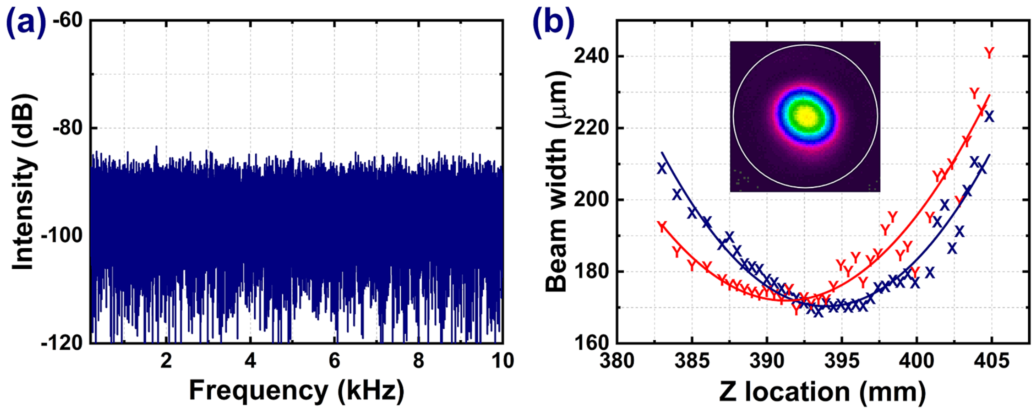

Figure 5. Output properties of the signal laser at the maximum output power in the fiber amplifier employing the bidirectional pumping scheme: (a) Fourier spectrum; (b) beam quality factor (the insert figure is beam profile at the location of $Z = 393.5$ mm).

of the fiber amplifier employing unidirectional pumping schemes (~2.82 and ~3.62 kW). In addition, the maximum injected backward pump power in the bidirectional pumping scheme is also close to that in the backward pumping scheme. Those two results could introduce two practical guidance in the design of high-power narrow-linewidth fiber amplifiers employing the bidirectional pumping scheme, when power scaling of the unidirectional pumping schemes is restricted by the TMI effect. Firstly, the practical power limit of a high-power narrow-linewidth fiber amplifier might be estimated through measuring the TMI effect of the fiber amplifier employing unidirectional pumping schemes. Secondly, the maximum launched backward pump power in the bidirectional pumping scheme could be obtained through the maximum injected pump power in the backward pumping scheme. Therefore, the output properties of the fiber amplifier employing unidirectional pumping schemes could provide practical guidance for the optimal design and potential exploration of high-power narrow-linewidth fiber amplifiers employing the bidirectional pumping scheme.

We might notice the obvious difference among the 3 dB spectral linewidth of the signal laser at the corresponding maximum output power in the three pumping schemes. To further reveal the difference, we have measured and calculated the 3 dB spectral linewidth of the signal laser at different output powers in the three pumping schemes. As shown in Figure 6, the overall changes for 3 dB spectral linewidth are irregular in the three cases. In particular, the 3 dB spectral linewidth ranges from approximately 0.41 nm to approximately 0.86 nm when the output power is over 4.5 kW. Thus, the 3 dB spectral linewidth might not be appropriate to characterize the spectral performance of high-power narrow-linewidth fiber amplifiers. For further consideration of the spectral wing broadening phenomenon, it might be useful to characterize the spectral purity of high-power narrow-linewidth fiber amplifiers through the 20 dB spectral linewidth or the power-ratio spectral linewidth[30].

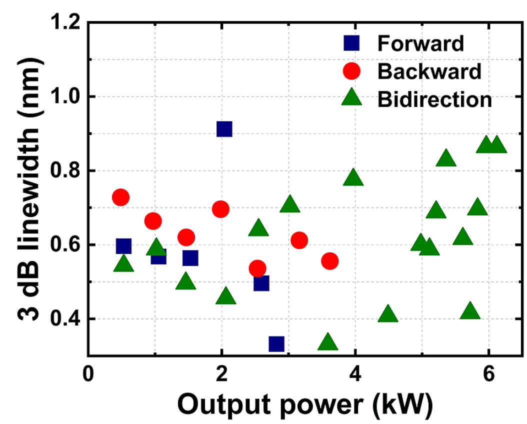

Figure 6. The 3 dB spectral linewidths of the signal laser at different output powers.

4. Conclusion

In this work, a more than 6 kW narrow-linewidth fiber laser with near-diffraction-limited beam quality has been reported based on a conventional all-fiberized YDF amplifier. Up to 6.12 kW fiber laser is achieved at a total pump power of 7.77 kW (3.17 kW forward pump and 4.6 kW backward pump) with the corresponding conversion efficiency of approximately 78.8%. At the maximum output power, the 3 dB spectral linewidth is approximately 0.86 nm, and the beam quality factor is $M_x^2 = 1.43$, $M_y^2 = 1.36$. To the best of our knowledge, this is the highest power ever reported in narrow-linewidth fiber lasers with near-diffraction-limited beam quality. Further comparisons among the fiber amplifier employing different pumping schemes indicate that the practical power limit of a high-power narrow-linewidth fiber amplifier could be close to the sum of the maximum output powers of the same fiber amplifier employing unidirectional pumping schemes. Overall, this work could provide a good reference for the optimal design and potential exploration of high-power narrow-linewidth fiber laser systems.

Acknowledgment

This work was supported by National Natural Science Foundation of China (NSFC) (62005313, 62035015) and Innovative Research Team in Natural Science Foundation of Hunan Province (2019JJ10005).

References

1. D. J. Richardson, J. Nilsson, and W. A. Clarkson, J. Opt. Soc. Am. B **27**, B63 (2010).
2. W. Shi, Q. Fang, X. Zhu, R. A. Norwood, and N. Peyghambarian, Appl. Opt. **53**, 6554 (2014).
3. M. N. Zervas and C. A. Codemard, IEEE J. Sel. Top. Quantum Electron. **20**, 219 (2014).
4. IPG Photonics Corporation, "IPG photonics successfully tests world's first 10 kilowatt single-mode production laser," http://www.ipgphotonics.com (2009).
5. B. Shiner, "The impact of fiber laser technology on the world wide material processing market," in *CLEO: Applications and Technology* (Optica Publishing Group, 2013), paper AF2J.1.
6. J. W. Dawson, M. J. Messerly, R. J. Beach, M. Y. Shverdin, E. A. Stappaerts, A. K. Sridharan, P. H. Pax, J. E. Heebner, C. W. Siders, and C. P. J. Barty, Opt. Express **16**, 13240 (2008).
7. J. Zhu, P. Zhou, Y. Ma, X. Xu, and Z. Liu, Opt. Express **19**, 18645 (2011).
8. M. N. Zervas, Opt. Express **27**, 19019 (2019).
9. T. Y. Fan, IEEE J. Sel. Top. Quantum Electron. **11**, 567 (2005).
10. Y. Zheng, Y. Yang, J. Wang, M. Hu, G. Liu, X. Zhao, X. Chen, K. Liu, C. Zhao, B. He, and J. Zhou, Opt. Express **24**, 12063 (2016).
11. Z. Liu, P. Ma, R. Su, R. Tao, Y. Ma, X. Wang, and P. Zhou, J. Opt. Soc. Am. B **34**, A7 (2016).
12. P. Ma, H. Xiao, W. Liu, H. Zhang, X. Wang, J. Leng, and P. Zhou, High Power Laser Sci. Eng. **9**, e45 (2021).
13. Z.-M. Huang, Q. Shu, R.-M. Tao, Q.-H. Chu, Y. Luo, D.-L. Yan, X. Feng, Y. Liu, W.-J. Wu, H.-Y. Zhang, H.-H. Lin, J.-J. Wang, and F. Jing, IEEE Photonics Technol. Lett. **33**, 1181 (2021).
14. C. X. Yu, O. Shatrovoy, T. Y. Fan, and T. F. Taunay, Opt. Lett. **41**, 5202 (2016).
15. Y. Xu, Q. Fang, Y. Qin, X. Meng, and W. Shi, Appl. Opt. **54**, 9419 (2015).
16. H. Shen, Q. Lou, Z. Quan, X. Li, Y. Yang, X. Chen, Q. Li, G. Bai, Y. Qi, B. He, and J. Zhou, Appl. Opt. **58**, 3053 (2019).
17. P. Ma, R. Tao, R. Su, X. Wang, P. Zhou, and Z. Liu, Opt. Express **24**, 4187 (2016).
18. S. Ren, W. Lai, G. Wang, W. Li, J. Song, Y. Chen, P. Ma, W. Liu, and P. Zhou, Opt. Express **30**, 7845 (2022).
19. A. V. Smith and J. J. Smith, Opt. Express **19**, 10180 (2011).
20. B. Ward, C. Robin, and I. Dajani, Opt. Express **20**, 11407 (2012).
21. R. Tao, X. Wang, and P. Zhou, IEEE J. Sel. Top. Quantum Electron. **24**, 0903319 (2018).
22. C. Jauregui, C. Stihler, and J. Limpert, Adv. Opt. Photonics **12**, 429 (2020).
23. K. R. Hansen and J. Lægsgaard, Opt. Express **22**, 11267 (2014).
24. R. Tao, R. Su, P. Ma, X. Wang, and P. Zhou, Laser Phys. Lett. **14**, 025101 (2017).
25. C. Shi, R. T. Su, H. W. Zhang, B. L. Yang, X. L. Wang, P. Zhou, X. J. Xu, and Q. S. Lu, IEEE Photonics J. **9**, 1502910 (2017).
26. H.-J. Otto, A. Klenke, C. Jauregui, F. Stutzki, J. Limpert, and A. Tünnermann, Opt. Lett. **39**, 2680 (2014).
27. Z. Zhang, X. Lin, G. Chen, L. Liao, Y. Xing, H. Li, J. Peng, N. Dai, and J. Li, IEEE Photonics J. **13**, 1501006 (2021).
28. N. Xia and S. Yoo, J. Lightwave Technol. **38**, 4478 (2020).
29. H. Wu, R. Li, H. Xiao, L. Huang, H. Yang, Z. Pan, J. Leng, and P. Zhou, Opt. Express **29**, 31337 (2021).
30. W. Liu, J. Song, P. Ma, H. Xiao, and P. Zhou, Photonics Res. **9**, 424 (2021).